Title

Time-Resolved Noncontrast Magnetic Resonance Perfusion Imaging of Paraspinal Muscles

Journal

Journal of Magnetic Resonance Imaging, 56(5)

ISSN

1053-1807

Authors

Miyazaki, Mitsue

Yamamoto, Asako

Malis, Vadim

et al.

Publication Date

2022-11-01

DOI

10.1002/jmri.28123

Peer reviewed

HHS Public Access

Author manuscript

J Magn Reson Imaging. Author manuscript; available in PMC 2023 November 01.

Published in final edited form as:

J Magn Reson Imaging. 2022 November ; 56(5): 1591–1599. doi:10.1002/jmri.28123.

Time-Resolved Noncontrast Magnetic Resonance Perfusion Imaging of Paraspinal Muscles

Mitsue Miyazaki, PhD[1], **Asako Yamamoto, MD**[2], **Vadim Malis, PhD**[1], **Sheronda Statum, MBA, DHA**[1,4], **Christine B. Chung, MD**[1,4], **Jesse Sozanski, MD**[3], **Won C. Bae, PhD**[1,4,*]

[1]Department of Radiology, University of California, San Diego, La Jolla, California, USA

[2]Department of Radiology, Teikyo University School of Medicine, Tokyo, Japan

[3]Department of Family Medicine, University of California, San Diego, La Jolla, California, USA

[4]Department of Radiology, VA San Diego Healthcare System, San Diego, California, USA

Abstract

Background: While evaluation of blood perfusion in lumbar paraspinal muscles is of interest in low back pain, it has not been performed using noncontrast magnetic resonance (MR) techniques.

Purpose: To introduce a novel application of a time-resolved, noncontrast MR perfusion technique for paraspinal muscles and demonstrate effect of exercise on perfusion parameters.

Study Type: Longitudinal.

Subjects: Six healthy subjects (27–48 years old, two females) and two subjects with acute low back pain (46 and 65 years old females, one with diabetes/obesity).

Field Strength/Sequence: 3-T, MR perfusion sequence.

Assessment: Lumbar spines of healthy subjects were imaged axially at L3 level with a tag-on and tag-off alternating inversion recovery arterial spin labeling technique that suppresses background signal and acquires signal increase ratio (SIR) from the in-flow blood at varying inversion times (TI) from 0.12 seconds to 3.5 seconds. SIR vs. TI data were fit to determine the perfusion metrics of peak height (PH), time to peak (TTP), mean transit time, apparent muscle blood volume (MBV), and apparent muscle blood flow (MBF) in iliocostal, longissimus, and multifidus. Imaging was repeated immediately after healthy subjects performed a 20-minute walk, to determine the effect of exercise.

Statistical Tests: Repeated measures analysis of variance.

Results: SIR vs. TI data showed well-defined leading and trailing edges, with sharply increasing SIR to TI of approximately 500 msec subsiding quickly to near zero around TI of 1500 msec. After exercise, the mean SIR at every TI increased markedly, resulting in significantly higher PH, MBV, and MBF (each $P < 0.001$ and $F > 28.9$), and a lower TTP ($P < 0.05$, $F = 4.5$), regardless of

*Address reprint requests to: W.C.B., 9427 Health Sciences Drive, San Diego, CA 92093, USA. wbae@ucsd.edu.

Conflict of Interest

Dr. Bae has a research funding from General Electric Healthcare and Dr. Miyazaki has a research funding from Canon Medical Systems. The remaining coauthors have no conflicts of interest.

the muscle. MBF increased 2- to 2.5-fold after exercise, similar to the expected increase in cardiac output, given the intensity of the exercise.

Data Conclusions: Feasibility of an MR perfusion technique for muscle perfusion imaging was demonstrated, successfully detecting significantly increased perfusion after exercise.

Level of Evidence: 1

Technical Efficacy Stage: 1

Low back pain is a serious health concern with often unclear etiology. Along with the pathology of intervertebral disks and vertebral bodies, paraspinal muscles are believed to play a significant role.[1] Muscular alterations including atrophy and increased fat infiltration,[2,3] increased muscle fatigue,[4] and decreased blood perfusion[5,6] have been found in low back pain subjects. Blood perfusion has been of particular interest in terms of integrative medicine, where the increased microcirculation in target muscles is regarded as a useful means to evaluate the peripheral effects of acupuncture.[7,8]

Blood flow in paraspinal muscles has been difficult to evaluate precisely. Currently available methods include laser-Doppler perfusion imaging[9–11] and near infrared spectrophotometry[12] to measure oxygen uptake. These work well for anatomies with shallow depths such as the hand but have limited penetration depths (mm to cm) to evaluate paraspinal muscles effectively.[9–11]

Magnetic resonance (MR) perfusion techniques based on arterial spin labeling (ASL), exploiting the protons in the arterial blood as intrinsic markers, have been used widely in the brain[13–15] and in other high-flow organs such as the heart,[16–18] kidney,[19–22] and lungs.[23] Relatively few studies report the use of ASL for the leg muscle,[24–26] and none in paraspinal muscles. Additionally, the past studies on muscle utilized continuous tagging such as pseudo-continuous ASL to determine the average perfusion. However, those were inherently not time-resolved and unable to determine the time-course of the perfusion signal change, crucial for detecting focal changes related to vascularity. Although techniques utilizing blood oxygen level-dependent MRI[3,27] have been used in the lower back, these have only provided indirect measures.

Time-resolved perfusion data provide additional clinical information regarding hemodynamics of a tissue. Initially described for brain imaging, a time-resolved perfusion curve can be analyzed to determine additional metrics including mean transit time (MTT), time to peak (TTP), cerebral (or muscular in case of muscle) blood volume, and cerebral blood flow.[28] These metrics can distinguish normal from ischemic tissues,[29,30] making them useful for stroke evaluation in the brain and for detecting focal myocardial infarction in the heart for example. The gold standard for perfusion imaging often utilizes contrast injection followed by imaging.[31,32] There are noncontrast time-resolved ASL techniques such as quantitative imaging of perfusion using a single subtraction[33] and flow-sensitive alternating inversion recovery[34]; however, these have somewhat ill-defined leading and trailing edges of the signal bolus, and none have been applied to the paraspinal muscles.

The goal of this feasibility study was to introduce a novel application of a time-resolved, noncontrast MR ASL perfusion technique for the evaluation of lumbar paraspinal muscles and to demonstrate the effect of exercise on perfusion parameters in a group of healthy volunteers.

Materials and Methods

This human subject study was approved by the institutional ethical committee (IRB registration number 200335). All procedures performed in this study involving human participants were compliant with the regulations of the Health Insurance Portability and Accountability Act (HIPAA).

Human Subjects

Six healthy, asymptomatic (i.e., no current or recent low back pain, self-reported), normal weight (body mass index [BMI] < 25) volunteers were recruited for this study (two females and four males, aged 36.0 ± 8.1 years old, range 27–48 years old). The healthy subjects had no known history of vascular diseases or conditions associated with vascular diseases such as diabetes. MR imaging was performed at rest (typically midday, without any exercise within the last 2 hours) and immediately after a 20 minutes of walking exercise (1.6–2.0 km, about 2000–3000 steps, resulting in a calorie burn of roughly 90–110 calories).

Additionally, two subjects with acute low back pain (new presentation within 3 weeks of MRI) were recruited. One was a 46-year-old female with type 2 diabetes (BMI of 36) and the other was a 65-year-old female with a normal BMI of 18.5–24.9 kg/m^2. These subjects were imaged at rest without exercise. Subject characteristics are provided in Table 1.

Exercise

To enhance overall blood flow to the body and to the paraspinal muscles, healthy subjects performed a 20 minutes long, continuous moderate walking outside the MR facility.

MR Imaging

Lumbar spine MRI was performed on a Vantage Galan 3-T scanner (Canon Medical Systems Corp., Tochigi, Japan) in a supine position sandwiched between the standard spine array coil on the posterior side and an Altas SPEEDER 16-ch array on the anterior side of the subject. Each subject was imaged with anatomic and perfusion sequences as given in Table 2. Anatomic images were used to identify and manually draw regions of interest (ROIs) for paraspinal muscles (performed by an musculoskeletal (MSK) radiologist using a custom Matlab routine) and to create overlaid color maps of perfusion parameters.

PERFUSION IMAGING.—Here, we propose an ASL technique using three-dimensional balanced steady-state free precession readout that reduce issues with often-used echo-planar imaging acquisition that is sensitive to B_0 inhomogeneity and motion artifacts. We utilized the tag-on and tag-off alternating inversion recovery using tag-on, selective IR (sel-IR) pulse and non-sel-IR pulse and tag-off (only non-sel-IR pulse) acquisitions and subtraction, as shown in Fig. 1a, with a goal to cancel the background signal and depict signal from

microvascularity in the muscles. The tag, 30-cm-thick, adiabatic IR pulse with a duration of about 200 msec, was applied on the aorta immediately superior and parallel to the imaging plane (Fig. 1b) to provide a tagged signal that is acquired at varying inversion times (TI) to determine the time-course of perfusion. We acquired a total of seven TIs between 120 msec and 3500 msec (when most of the signal has subsided), using respiratory gating. We chose an axial imaging plane (a 62.4-mm slab, 24 slices of 2.6 mm thickness) with a voxel size of 1.56 (phase encoding) × 1.37 (readout) × 2.6 (slice encoding) mm^3 through the L3 vertebral body (Fig. 1c), to capture major lumbar paraspinal muscles including iliocostal, longissimus, and multifidus on the left and right sides (Fig. 2a).

MR Perfusion Analysis

For each TI, tag-on and tag-off images were subtracted (Fig. 1c) and then divided by tag-off images to determine the signal increase ratio (SIR) at each voxel (Eq. 1):

$$\mathrm{SIR} = \frac{\mathrm{SI}_{\mathrm{TagOn}} - \mathrm{SI}_{\mathrm{TagOff}}}{\mathrm{SI}_{\mathrm{TagOff}}} \quad (1)$$

To reduce noise, we then created stack-averaged images (Fig. 2b–f) to show the time-course of tag-signal over varying TIs. We chose six ROIs encompassing paraspinal muscles (Fig. 2a) to determine the time-course of SIR vs. TI time (Fig. 3a). Using a gamma variate function,[35] the data were fit to a smooth perfusion curve (Fig. 3a, orange line), and the curve was further analyzed to determine five perfusion metrics of peak height (PH), TTP, MTT (width at half of the PH), apparent muscle blood volume (MBV; area under the curve), and apparent muscle blood flow (MBF; MBV divided by MTT), following the convention.[36]

To determine reproducibility, one of the subjects was reimaged 6 months later under similar setting as the preexercise condition. Average SIR curves and perfusion metrics (Fig. 3b) were determined at each time point by averaging values from the six ROIs.

In addition to ROI analysis, we performed the perfusion fitting for each voxel of the stack-averaged signal image (Fig. 2b–f) to create five colormaps (Fig. 4) showing the spatial distribution of the aforementioned perfusion metrics of PH, TTP, MTT, MBV, and MTT.

Statistics

Using repeated measures analysis of variance (ANOVA), effects of exercise (repeated factor) and ROI on the mean perfusion metrics were assessed, after a log transformation to address nonnormality of the data. A commercially available software was used (Systat 12, Systat Software, San Jose, CA, USA). Statistical significance was set at a $P < 0.05$. Power analysis was performed using G*Power software.[37]

Results

Time-Course of Perfusion Enhancement

Using our noncontrast MR perfusion technique, spatiotemporal distribution of a tagged perfusion signal was visualized (Fig. 2b–f). Perfusion signal increased sharply to a peak near

TI of 500 msec (Fig. 2c) and subsided quickly to near zero values or baseline around TI of 1500 msec (Fig. 2e), demonstrating a well-defined leading and trailing edges of the signal bolus as well as revealing spatial variations such as hotspots suggesting focally high and persistent perfusion (Fig. 2d, arrow), which could potentially be caused by muscle injury or other vascular conditions. When averaged for each ROI, SIR vs. TI (Fig. 3) followed the same trend, increasing to a peak near TI of 500 msec then decreasing to less than 10% by 2000 msec. Perfusion fitting with gamma variate function was generally good (Fig. 3a, orange line), following the raw data points closely (Fig. 3a, blue circles) and facilitating determination of perfusion metrics. Reproducibility, though not statistically evaluated, was also good, showing a close agreement in SIR vs. TI curves as well as perfusion metrics (Fig. 3b) when acquired 6 months apart.

Effect of Exercise

Figure 5 shows the average SIR of the left multifidus muscle for all six subjects, before (Fig. 5a) and after (Fig. 5b) exercise. After exercise, we see a marked increase in mean SIR at every TI, though there was a large person-to-person variability contributing to a large confidence interval. After curve fitting, the mean PH was higher after exercise (from 69 ± 33% to 156 ±90%), and along with MBV and MBF.

Consistent with the SIR, the mean perfusion metrics for each ROI (Fig. 6a) also showed marked changes with exercise. PH (Fig. 6b) was significantly higher after exercise ($P < 0.001$, $F = 29.1$) regardless of the muscle ROI ($P = 0.99$, $F = 0.07$). In addition, after exercise, time-to-peak (Fig. 6c) was significantly lower ($P < 0.05$, $F = 4.5$), apparent MBV (Fig. 6d) was significantly higher ($P < 0.001$, $F = 28.9$), and apparent MBF (Fig. 6e) was significantly higher ($P < 0.001$, $F = 30.4$), all regardless of the ROI (each $P > 0.9$, $F < 0.1$). MTT (Fig. 6f) was the only perfusion metric that was not significantly different before vs. after exercise ($P = 0.6$, $F = 0.5$). There was no significant interaction between exercise and ROI (all $P > 0.9$, $F < 0.1$).

Feasibility in Patients

To demonstrate clinical feasibility of the technique, we determined perfusion metrics in two low back pain subjects. In comparison with the values in healthy subjects before exercise, PH and MBF metrics were generally lower, while the time metrics were higher (Fig. 7a). However, these values were not compared statistically due to a small sample size.

Although not specifically used for the analysis, perfusion color maps (Figs. 4 and 7) also provided useful visual information to assess regional differences in perfusion metrics. Focal areas with hyper or hypo perfusion can be depicted using the maps, which may help to localize regions of inflammation or perfusion deficiency. In subjects with low back pain, highly heterogeneous colormaps of MBF (Fig. 7b and c) could be seen in comparison with that from a healthy subject (Fig. 4e).

Discussion

Despite an important role of paraspinal muscles in low back pain and an interest in measuring MBF, relatively little progress has been made in the area of noncontrast MR

imaging. This study, for the first time in our knowledge, describes the feasibility of an ASL technique to determine the time-course of blood perfusion in individual paraspinal muscles as well as quantitative perfusion metrics. We found that our technique acquired well-defined time-resolved perfusion curves with distinct leading and trailing edges, which also made quantification of perfusion metrics, eg, calculation of MTT from width of the curve at half maximum, relatively trivial. Note that our perfusion curves have clear tailing or signal return to the baseline which is not possible with contrast-enhanced methodologies due to the contrast circulating in the body and not washing out quickly.

The results of altered perfusion after the exercise demonstrated sensitivity of our technique to physiologic changes and future potential for clinical and research applications. While the perfusion metrics varied from person-to-person, after exercise, there was a consistent increase in SIR at most TI times (Fig. 5) and corresponding increase in PH, MBV, and MBF values (Fig. 6), as well as a slight decrease in TTP. The mean increase in MBF was roughly 2-fold. These results are consistent with studies on exercise physiology. Based on the compendium of physical activities,[38] a brisk 20-minute walk (at 2.5 mph) has a metabolic equivalent (MET) value of 3.0, compared to the resting state which has an MET of 1.3. Cardiac output is increased proportionally[39] and one would expect a 2.3-fold increase in blood flow to the entire body. Our results of MBF (Fig. 6e) suggested 2.0-to-2.5-fold increases in different ROIs after the exercise, in close agreement with the expected increase in blood flow based on the exercise physiology. We did not find differences in MBF between ROIs, which also appear consistent with relatively similar capillary density between the paraspinal muscles in young and presumably normal subjects.[40]

Our early-stage study has several limitations. While our results appear valid in light of the known effect of walking on cardiac output,[39] additional validation against reference technologies could inspire stronger confidence in the MR technique. Optical methods such as laser-Doppler perfusion imaging[9–11] and near infrared spectrophotometry[6,12] could be used to validate MR perfusion findings in other compatible anatomies such as the hand. Contrast-enhanced imaging[41–43] could also be used to validate the present results but requires contrast injections, which maybe undesirable in healthy volunteers. One limitation of our technique is that it determines perfusion in descriptive terms, which are indirect descriptors of perfusion. However, this is routinely performed in contrast-enhanced imaging studies and have been shown to be reproducible.[44] Another limitation of our technique is that multiple imaging series, each up to 2 minutes long, is currently required to obtain the full time-resolved data. This could be shortened considerably in the future by reducing the number of slices, optimizing or reducing number of TI, and creating a dedicated sequence that eliminates separate acquisition at each TI. Lastly, although the number of subjects used in this study was low, given a large exercise effect, the perfusion metrics before and after exercise could be discerned with high statistical power.

Future work may include studies of greater number of low back pain subjects to determine the role paraspinal muscle play in pain and to determine whether muscle perfusion changes can indicate a response to therapy[6] or improvement in clinical condition. While inconclusive, the data on two symptomatic subjects (including a diabetic subject with likely impaired blood flow) were promising, suggesting the feasibility of the technique and

justifying additional studies to studies blood flow in paraspinal muscles in low back pain subjects. Our three-dimensional technique is particularly useful for precise localization of areas of deficiency and response. Additionally, the technique described here can potentially be applied to other skeletal muscles with peripheral artery disease[45,46] or joints with inflammatory disease.[47,48]

In conclusion, our study demonstrated the feasibility of a novel application of an ASL technique with desired features for muscle perfusion imaging, including spatiotemporal resolution and well-defined leading and trailing edges of the temporal signal. Effect of exercise was also demonstrated, with a significant increase in blood flow commensurate with the exercise intensity. While additional studies are needed, the techniques presented here could be useful in combination with routine MR evaluations of the low back and other skeletal muscles.

Acknowledgments

The authors thank Canon Medical Systems Japan for research support. Research reported in this publication was supported in parts by the National Institute of Arthritis and Musculoskeletal and Skin Diseases of the National Institutes of Health under Award Number R01 AR066622 and P30 AR073761 in support of Dr. Bae and Award Number 5I01CX000625 (Project ID: 1161961) from the Clinical Science Research & Development of the Veterans Affairs Office of Research and Development in support of Dr. Chung. The content is solely the responsibility of the authors and does not necessarily represent the official views of the National Institutes of Health or Veterans Affairs.

References

1. Tsuang YH, Novak GJ, Schipplein OD, Hafezi A, Trafimow JH, Andersson GB. Trunk muscle geometry and centroid location when twisting. J Biomech 1993;26(4–5):537–546. [PubMed: 8478355]
2. Goubert D, Oosterwijck JV, Meeus M, Danneels L. Structural changes of lumbar muscles in non-specific low Back pain: A systematic review. Pain Physician 2016;19(7):E985–E1000. [PubMed: 27676689]
3. Wan Q, Lin C, Li X, Zeng W, Ma C. MRI assessment of paraspinal muscles in patients with acute and chronic unilateral low back pain. Br J Radiol 2015;88(1053):20140546. [PubMed: 26105517]
4. Hao Z, Xie L, Wang J, Hou Z. Spatial distribution and asymmetry of surface electromyography on lumbar muscles of soldiers with chronic low Back pain. Pain Res Manag 2020;2020:6946294. [PubMed: 33163126]
5. Sakai Y, Matsuyama Y, Ishiguro N. Intramuscular oxygenation of exercising trunk muscle in elderly persons. J Lumbar Spine Disord 2005;11:145–156.
6. Sakai Y, Matsuyama Y, Nakamura H, et al. The effect of muscle relaxant on the paraspinal muscle blood flow: A randomized controlled trial in patients with chronic low back pain. Spine (Phila Pa 1976) 2008;33(6): 581–587. [PubMed: 18344850]
7. Moffet HH. How might acupuncture work? A systematic review of physiologic rationales from clinical trials. BMC Complement Altern Med 2006;6:25. [PubMed: 16824230]
8. Litscher G Bioengineering assessment of acupuncture, part 2: Monitoring of microcirculation. Crit Rev Biomed Eng 2006;34(4):273–294. [PubMed: 17206916]
9. Murray AK, Herrick AL, King TA. Laser Doppler imaging: A developing technique for application in the rheumatic diseases. Rheumatology (Oxford) 2004;43(10):1210–1218. [PubMed: 15226515]
10. Fredriksson I, Larsson M, Stromberg T. Measurement depth and volume in laser Doppler flowmetry. Microvasc Res 2009;78(1):4–13. [PubMed: 19285089]
11. Min S, Lee H, Kim SY, et al. Local changes in microcirculation and the analgesic effects of acupuncture: A laser Doppler perfusion imaging study. J Altern Complement Med 2015;21(1):46–52. [PubMed: 25354241]

12. Demoulin C, Crielaard JM, Vanderthommen M. Spinal muscle evaluation in healthy individuals and low-back-pain patients: A literature review. Joint Bone Spine 2007;74(1):9–13. [PubMed: 17174584]
13. Detre JA, Leigh JS, Williams DS, Koretsky AP. Perfusion imaging. Magn Reson Med 1992;23(1):37–45. [PubMed: 1734182]
14. Kim SG. Quantification of relative cerebral blood flow change by flow-sensitive alternating inversion recovery (FAIR) technique: Application to functional mapping. Magn Reson Med 1995;34(3):293–301. [PubMed: 7500865]
15. Alsop DC, Detre JA. Multisection cerebral blood flow MR imaging with continuous arterial spin labeling. Radiology 1998;208(2):410–416. [PubMed: 9680569]
16. Williams DS, Grandis DJ, Zhang W, Koretsky AP. Magnetic resonance imaging of perfusion in the isolated rat heart using spin inversion of arterial water. Magn Reson Med 1993;30(3):361–365. [PubMed: 8412609]
17. Poncelet BP, Koelling TM, Schmidt CJ, et al. Measurement of human myocardial perfusion by double-gated flow alternating inversion recovery EPI. Magn Reson Med 1999;41(3):510–519. [PubMed: 10204874]
18. Miyazaki M, Zhou X, Hoshino T, Yokoyama K, Ishimura R, Nitatori T. Non-contrast myocardial perfusion using a novel 4D magnetic resonance arterial spin labeling technique: Initial experience. Microvasc Res 2015;98:94–101. [PubMed: 25645290]
19. Williams DS, Zhang W, Koretsky AP, Adler S. Perfusion imaging of the rat kidney with MR. Radiology 1994;190(3):813–818. [PubMed: 8115632]
20. Wang JJ, Hendrich KS, Jackson EK, Ildstad ST, Williams DS, Ho C. Perfusion quantitation in transplanted rat kidney by MRI with arterial spin labeling. Kidney Int 1998;53(6):1783–1791. [PubMed: 9607213]
21. Takahashi J, Ohmoto-Sekine Y, Yoshida T, Miyazaki M. Comparison of axial and coronal acquisitions by non-contrast-enhanced renal 3D MR angiography using flow-in time-spatial labeling inversion pulse. Magn Reson Mater Phy 2020;33(1):95–102.
22. Shonai T, Takahashi T, Ikeguchi H, Miyazaki M, Amano K, Yui M. Improved arterial visibility using short-tau inversion-recovery (STIR) fat suppression in non-contrast-enhanced time-spatial labeling inversion pulse (time-SLIP) renal MR angiography (MRA). J Magn Reson Imaging 2009;29(6):1471–1477. [PubMed: 19472424]
23. Mai VM, Hagspiel KD, Altes T, Goode AR, Williams MB, Berr SS. Detection of regional pulmonary perfusion deficit of the occluded lung using arterial spin labeling in magnetic resonance imaging. J Magn Reson Imaging 2000;11(2):97–102. [PubMed: 10713940]
24. Raynaud JS, Duteil S, Vaughan JT, et al. Determination of skeletal muscle perfusion using arterial spin labeling NMRI: Validation by comparison with venous occlusion plethysmography. Magn Reson Med 2001; 46(2):305–311. [PubMed: 11477634]
25. Frank LR, Wong EC, Haseler LJ, Buxton RB. Dynamic imaging of perfusion in human skeletal muscle during exercise with arterial spin labeling. Magn Reson Med 1999;42(2):258–267. [PubMed: 10440950]
26. Schewzow K, Fiedler GB, Meyerspeer M, et al. Dynamic ASL and T2-weighted MRI in exercising calf muscle at 7 T: A feasibility study. Magn Reson Med 2015;73(3):1190–1195. [PubMed: 24752959]
27. Huang Y, Wei J, Han D, et al. Muscular blood oxygen level-dependent MRI is beneficial to evaluate effectiveness of an exercise prescription. Ann Transl Med 2021;9(6):470. [PubMed: 33850867]
28. Zaharchuk G Theoretical basis of hemodynamic MR imaging techniques to measure cerebral blood volume, cerebral blood flow, and permeability. AJNR Am J Neuroradiol 2007;28(10):1850–1858. [PubMed: 17998415]
29. Branch KR, Haley RD, Bittencourt MS, Patel AR, Hulten E, Blankstein R. Myocardial computed tomography perfusion. Cardiovasc Diagn Ther 2017;7(5):452–462. [PubMed: 29255689]
30. Wang T, Su H, Gu J, Chen Q, Xu Q, Chen BT. Evaluation of skeletal muscle perfusion in a canine hind limb ischemia model using CT perfusion imaging. Diagn Interv Radiol 2020;26(1):28–33. [PubMed: 31650969]

31. Weber MA, Krix M, Delorme S. Quantitative evaluation of muscle perfusion with CEUS and with MR. Eur Radiol 2007;17(10):2663–2674. [PubMed: 17453217]
32. Leppek R, Hoos O, Sattler A, et al. MR-imaging of lower leg muscle perfusion. Herz 2004;29(1):32–46. [PubMed: 14968340]
33. Wong EC, Buxton RB, Frank LR. Quantitative imaging of perfusion using a single subtraction (QUIPSS and QUIPSS II). Magn Reson Med 1998;39(5):702–708. [PubMed: 9581600]
34. Kim SG, Tsekos NV. Perfusion imaging by a flow-sensitive alternating inversion recovery (FAIR) technique: Application to functional brain imaging. Magn Reson Med 1997;37(3):425–435. [PubMed: 9055234]
35. Chan AA, Nelson AJ. Simplified gamma-variate fitting of perfusion curves. IEEE International Symposium on Biomedical Imaging: Nano to Macro, Vol 2. Arlington, VA USA: Institute of Electrical and Electronics Engineers; 2004. p 1067–1070.
36. Copen WA, Schaefer PW, Wu O. MR perfusion imaging in acute ischemic stroke. Neuroimaging Clin N Am 2011;21(2):259–283. [PubMed: 21640299]
37. Faul F, Erdfelder E, Lang AG, Buchner A. G*Power 3: A flexible statistical power analysis program for the social, behavioral, and biomedical sciences. Behav Res Methods 2007;39(2):175–191. [PubMed: 17695343]
38. Ainsworth BE, Haskell WL, Herrmann SD, et al. 2011 compendium of physical activities: A second update of codes and MET values. Med Sci Sports Exerc 2011;43(8):1575–1581. [PubMed: 21681120]
39. Laughlin MH. Effects of exercise training on coronary circulation: Introduction. Med Sci Sports Exerc 1994;26(10):1226–1229. [PubMed: 7528317]
40. Jorgensen K, Nicholaisen T, Kato M. Muscle fiber distribution, capillary density, and enzymatic activities in the lumbar paravertebral muscles of young men, Significance for isometric endurance. Spine (Phila Pa 1976) 1993;18(11):1439–1450. [PubMed: 8235814]
41. Krix M, Weber MA, Krakowski-Roosen H, et al. Assessment of skeletal muscle perfusion using contrast-enhanced ultrasonography. J Ultrasound Med 2005;24(4):431–441. [PubMed: 15784761]
42. Duerschmied D, Olson L, Olschewski M, et al. Contrast ultrasound perfusion imaging of lower extremities in peripheral arterial disease: A novel diagnostic method. Eur Heart J 2006;27(3):310–315. [PubMed: 16308326]
43. Thompson RB, Aviles RJ, Faranesh AZ, et al. Measurement of skeletal muscle perfusion during postischemic reactive hyperemia using contrast-enhanced MRI with a step-input function. Magn Reson Med 2005;54(2):289–298. [PubMed: 16032661]
44. Ng CS, Raunig DL, Jackson EF, et al. Reproducibility of perfusion parameters in dynamic contrast-enhanced MRI of lung and liver tumors: Effect on estimates of patient sample size in clinical trials and on individual patient responses. AJR Am J Roentgenol 2010;194(2):W134–W140. [PubMed: 20093564]
45. Gimnich OA, Holbrook J, Belousova T, et al. Relation of magnetic resonance imaging based arterial signal enhancement to markers of peripheral artery disease. Am J Cardiol 2021;140:140–147. [PubMed: 33144163]
46. Englund EK, Langham MC. Quantitative and dynamic MRI measures of peripheral vascular function. Front Physiol 2020;11:120. [PubMed: 32184733]
47. Ferrell WR, Sturrock RD, Mallik AK, Abbot NC, Lockhart JC, Edmondson WD. Laser Doppler perfusion imaging of proximal interphalangeal joints in patients with rheumatoid arthritis. Clin Exp Rheumatol 1996;14(6):649–652. [PubMed: 8978960]
48. Ferrell WR, Balint PV, Egan CG, Lockhart JC, Sturrock RD. Metacarpophalangeal joints in rheumatoid arthritis: Laser Doppler imaging—initial experience. Radiology 2001;220(1):257–262. [PubMed: 11426007]

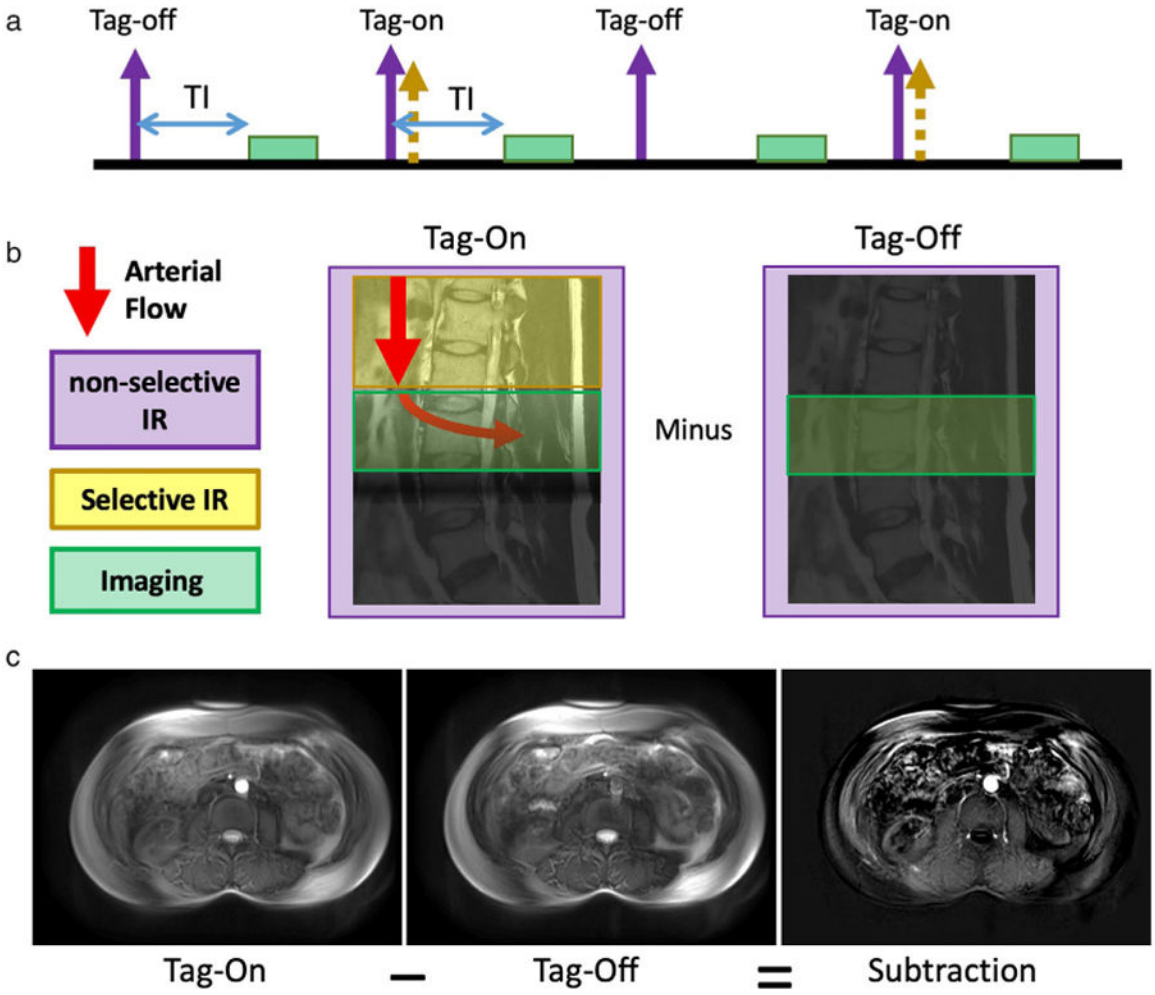

FIGURE 1:

(**a**) Tag-on and tag-off alternating inversion recovery (TAIR) technique. Tag-on is a spatial-selective IR (sel-IR) pulse and tag-off means only the non-sel-IR pulse is applied. The inversion time (TI) period is between the sel-IR pulse and image acquisition. (**b**) Schematic of arterial flow and locations of the tag and imaging slab. (**c**) Subtraction of tag-off from tag-on provides tagged blood that moved from outside of the tag region. Background signal is subtracted out at all TI times. Shown here are stack-averaged image from a subject before exercise acquired at TI of 1000 msec.

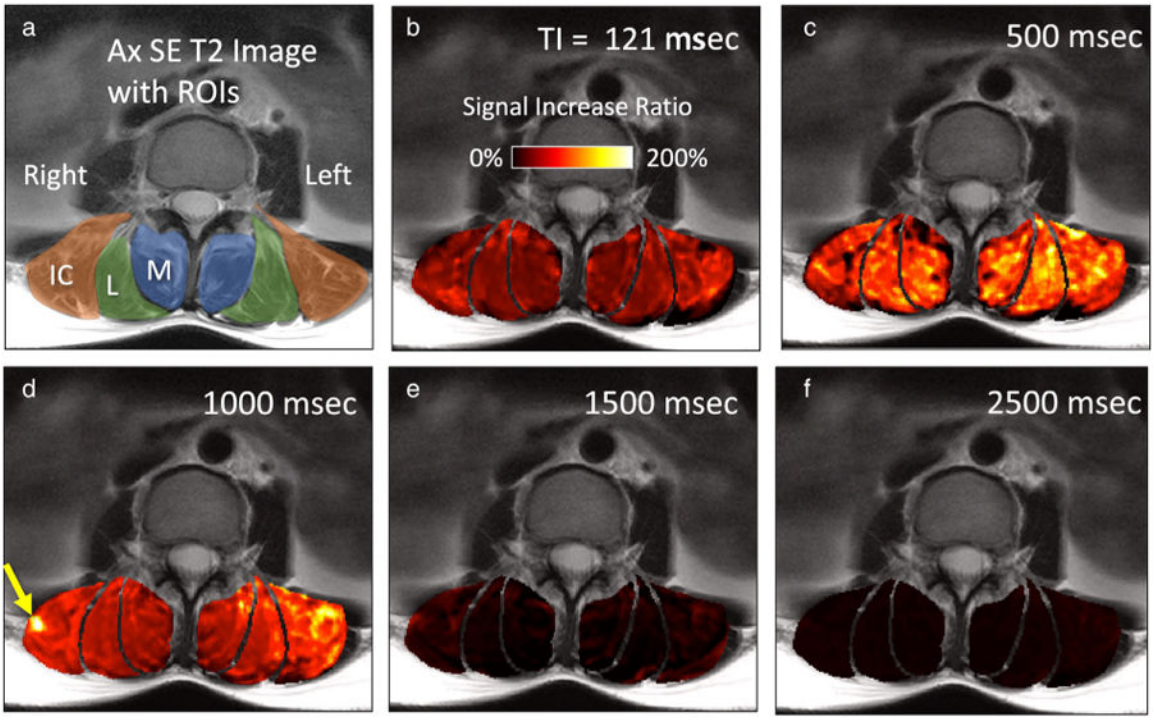

FIGURE 2:

Preexercise perfusion images from a healthy 40-year-old female volunteer. (**a**) Axial spin echo showing paraspinal muscles of iliocostal (IC), longissimus (L), and multifidus (M) on the left and right sides. (**b–f**) Perfusion images showing inversion time-dependent signal increase ratio (SIR). Note spatial variations in the SIR, including focal hyper-enhancement (d, arrow).

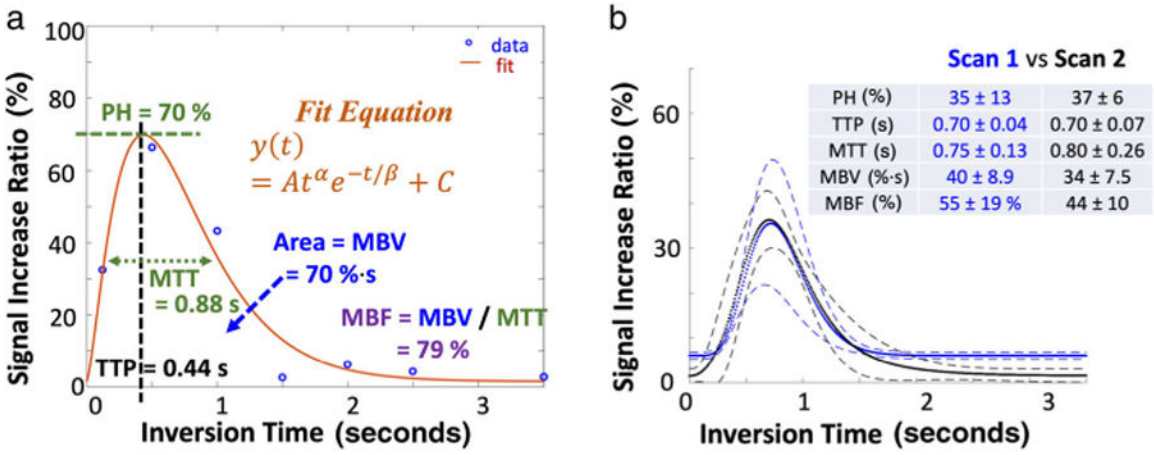

FIGURE 3:

(**a**) Curve fitting of signal increase ratio vs. inversion time data using a gamma variate function (orange line) followed by descriptive analyses to determine five perfusion metrics of peak height (PH), time to peak (TTP), mean transit time (MTT), apparent muscle blood volume (MBV), and apparent muscle blood flow (MBF). (**b**) One subject was imaged at two different times, 6 months apart. The mean perfusion curve (blue and black lines) as well as perfusion metrics of six regions of interest were similar, demonstrating the reproducibility of the technique.

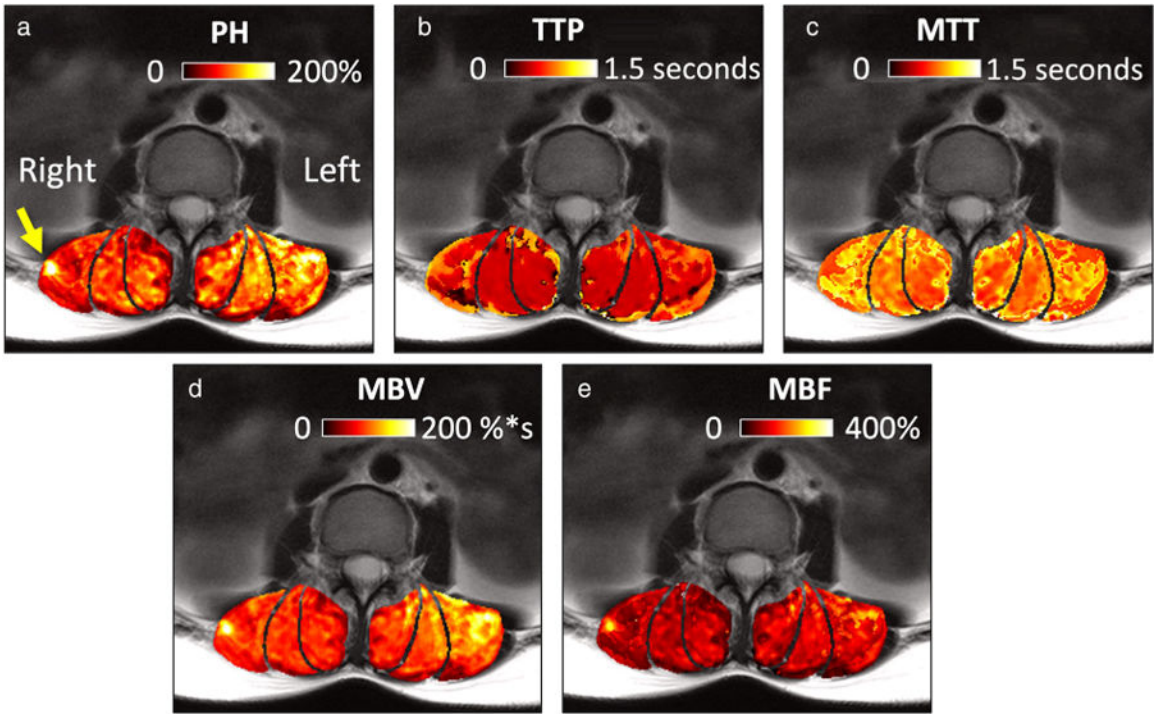

FIGURE 4:

Color maps of five perfusion metrics of (**a**) peak height (PH), (**b**) time to peak (TTP), (**c**) mean transit time (MTT), (**d**) apparent muscle blood volume (MBV), and (**e**) apparent muscle blood flow (MBF), from a healthy 40-year-old female subject. Note spatial variations in the values, such as generally higher PH values (a) on the left side, along with focally high value on the right side (arrow).

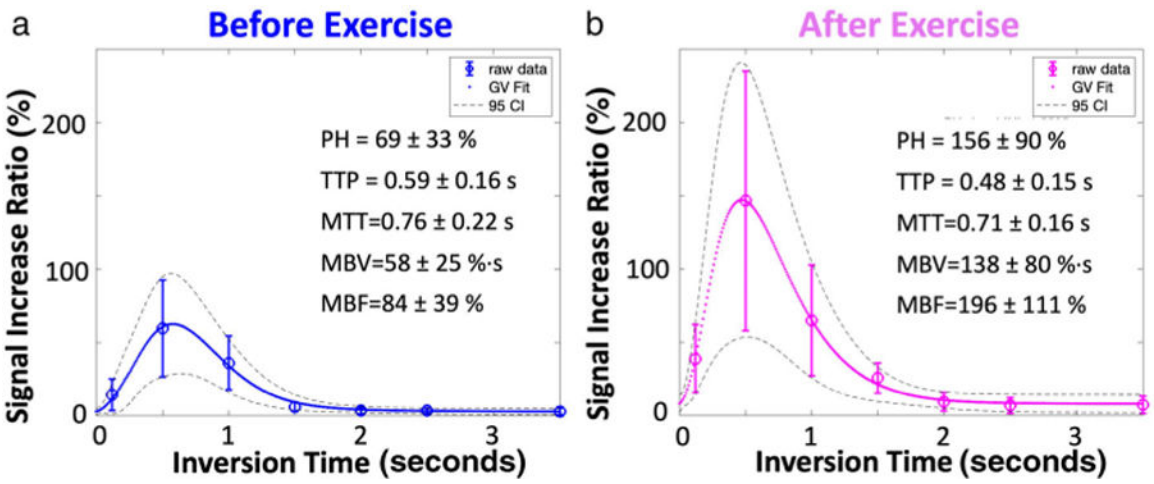

FIGURE 5:

Mean perfusion curves of signal increase ratio vs. inversion time (TI), before (**a**) and after (**b**) a 20-minute walk exercise in six healthy subjects, along with the mean perfusion metrics, in the left multifidus muscle. A marked increase in the magnitude was observed after the exercise, which also resulted in similar increases in many of the perfusion metrics.

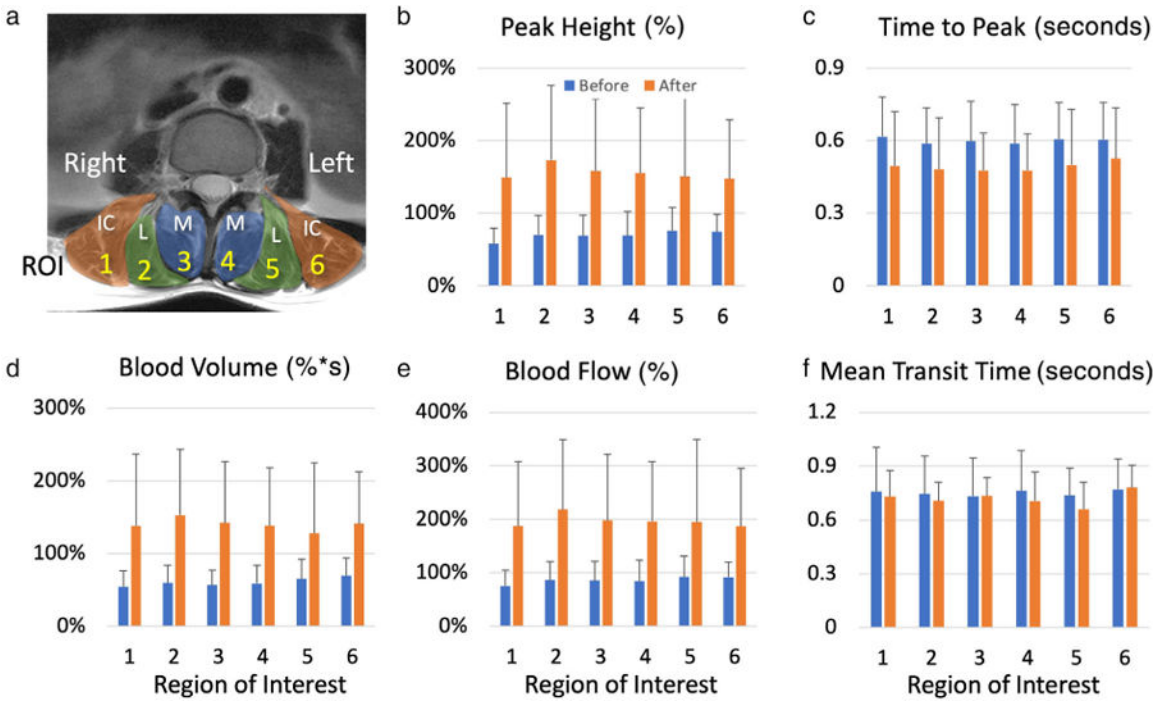

FIGURE 6:

Mean and standard deviation of the perfusion metrics in six healthy subjects, in each region of interest (ROI) of iliocostal (IC), longissimus (L), and multifidus (M) muscles on the left and right sides (**a**). After exercise, there was a significant increase in (**b**) peak height, (**d**) apparent muscle blood volume, and (**e**) apparent muscle blood flow (each $P < 0.001$), while (**c**) time to peak showed a decrease ($P < 0.05$). There was no significant difference in (**f**) mean transit time. There was no significant difference between the ROIs.

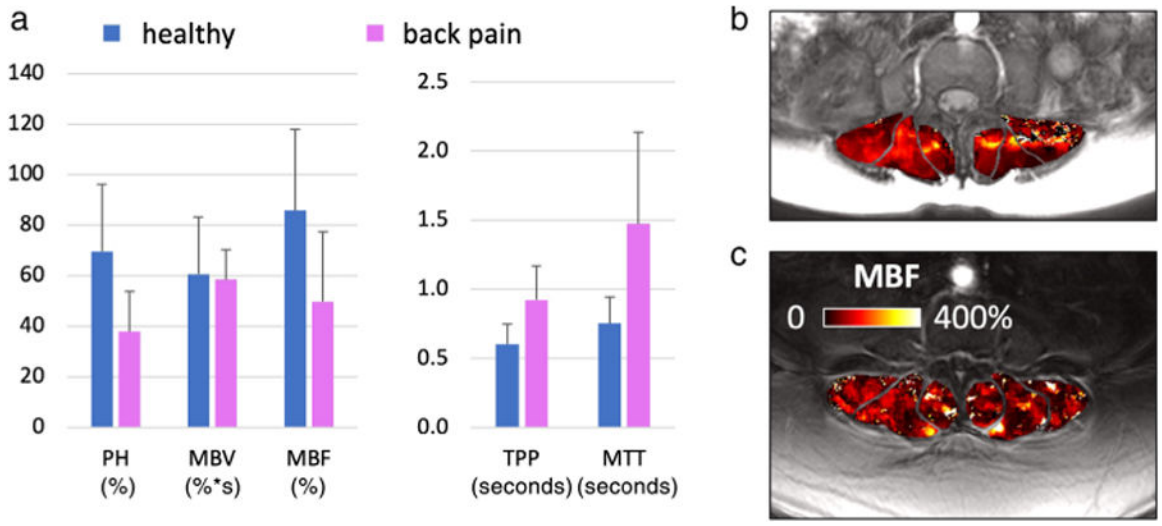

FIGURE 7:

(**a**) Perfusion metrics (mean of subjects and regions of interest [ROIs]) in six healthy and two low back pain subjects, before exercise. Both 64-year-old normal weight female (**b**) and 46-year-old diabetic/obese female (**c**) subjects exhibited heterogeneity in the colormaps of muscle blood flow. Peak height (PH), time to peak (TTP), mean transit time (MTT), apparent muscle blood volume (MBV), and apparent muscle blood flow (MBF).

TABLE 1.

Subject Characteristics

Group	ID#	Sex	Age (years)	Height (cm)	Weight (kg)	BMI (kg/m^2)	Resting HR (bpm)
Healthy	1	F	40	165	55	20.3	68
	2	M	27	176	77	24.9	80
	3	M	48	173	74	24.6	60
	4	M	40	173	68	22.7	55
	5	M	33	185	79	23.1	45
	6	F	28	168	59	20.9	62
Low back pain	7	F	65	156	58	23.8	52
	8	F	46	165	98	35.8	76

BMI = body mass index; HR = heart rate; bpm = beats per minute.

TABLE 2.

Scanning Parameters for the MR Sequences Used in This Study

Sequence	Plane	TR (msec)	TE (msec)	TI (seconds)	Matrix (Ph × RO)	Thick (mm)	# of slices	FOV (mm)	Time (minutes: seconds)
FSE T2w	Ax	3650	120	N/A	320 × 320	3	50	180	3:09
FSE T2w	Sag	3650	120	N/A	320 × 320	3	30	200	2:06
Perfusion	Ax	4.8	2.4	0.12, 0.5, 1.0, 1.5, 2.0, 2.5, 3.5	224 × 256	2.6	24	350	2:03

MR = magnetic resonance; FSE T2w = fast spin echo T2 weighted; Ax = axial; Sag = sagittal; TR = repetition time; TE = echo time; TI = inversion time; Ph = number of phase encoding; RO = number of frequency encoding; Thick = slice thickness; FOV = field of view; N/A = not applicable.